Orientation and Interaction of Oblique Cylindrical Inclusions Embedded in a Lipid Monolayer: A Theoretical Model for Viral Fusion Peptides

Yonathan Kozlovsky,* Joshua Zimmerberg,† and Michael M. Kozlov*
*Department of Physiology and Pharmacology, Sackler Faculty of Medicine, Tel Aviv University, 69978 Tel Aviv, Israel; and
†Laboratory of Cellular and Molecular Biophysics, National Institute of Child Health and Human Development, National Institutes of Health, Bethesda, Maryland USA

ABSTRACT We consider the elastic behavior of flat lipid monolayer embedding cylindrical inclusions oriented obliquely with respect to the monolayer plane. An oblique inclusion models a fusion peptide, a part of a specialized protein capable of inducing merger of biological membranes in the course of fundamental cellular processes. Although the crucial importance of the fusion peptides for membrane merger is well established, the molecular mechanism of their action remains unknown. This analysis is aimed at revealing mechanical deformations and stresses of lipid monolayers induced by the fusion peptides, which, potentially, can destabilize the monolayer structure and enhance membrane fusion. We calculate the deformation of a monolayer embedding a single oblique inclusion and subject to a lateral tension. We analyze the membrane-mediated interactions between two inclusions, taking into account bending of the monolayer and tilt of the hydrocarbon chains with respect to the surface normal. In contrast to a straightforward prediction that the oblique inclusions should induce tilt of the lipid chains, our analysis shows that the monolayer accommodates the oblique inclusion solely by bending. We find that the interaction between two inclusions varies nonmonotonically with the interinclusion distance and decays at large separations as square of the distance, similar to the electrostatic interaction between two electric dipoles in two dimensions. This long-range interaction is predicted to dominate the other interactions previously considered in the literature.

INTRODUCTION

A biological membrane binds multiple proteins, which play a fundamental biochemical and physiological role. A part of these proteins is totally or partially hydrophobic and, consequently, is embedded into the lipid matrix. Besides specific physiological and biochemical functions (see, e.g., Sackmann, 1995), the integral proteins affect the mechanical properties of the membrane generating deformations and, possibly, rearrangements of the lipid matrix (Epand, 1998). In turn, the membrane deformations can mediate effective interactions between the integral proteins in the membrane plane and influence the protein conformation (Huang, 1986).

The important group of integral fusion proteins is represented by the so-called fusion peptides, which constitute fragments of large membrane proteins mediating biological membrane fusion (see, e.g., Epand, 1998; Skehel and Wiley, 2000). In the best-investigated cases of the proteins responsible for fusion of influenza and HIV viruses with the cell membranes (Skehel and Wiley, 2000), the fusion peptide is a short (~20 residues) hydrophobic N-terminal fragment of the extracellular part of the proteins. The ability of the whole protein to induce fusion is critically dependent upon the structure of the fusion peptide and its proper insertion into the target membrane (see for review Cohen and Melikyan, 2001). Moreover, isolated fusion peptides (separated from the body of the native protein) have been shown to mediate fusion of synthetic lipid bilayers (liposomes) (Davies et al., 1998; Epand et al., 1994; Epand and Epand, 1994).

Although it is generally accepted that the fusion peptides can mediate membrane fusion by inducing local structural changes in the lipid monolayer structure, the mechanism of this phenomenon remains unknown. Recently, a considerable effort has been undertaken to understand physics of lipid monolayers containing proteins (Aranda-Espinoza et al., 1996; Bohinc et al., 2003; Dan et al., 1993; Fattal and Benshaul, 1993, 1995; Fournier, 1999; Goulian, 1996; Goulian et al., 1993; Helfrich and Weikl, 2001; Netz and Pincus, 1995; Park and Lubensky, 1996; Weikl et al., 1998). In all these works the proteins were modeled as axisymmetric inclusions having a shape of cylindrical rods whose length is different from the thickness of the bilayer (Aranda-Espinoza et al., 1996; Dan et al., 1993; Fattal and Benshaul, 1993; Huang, 1986), conical (Weikl et al., 1998), or barrel-like (Fournier, 1999) molecules. At the same time, the fusion peptides insert into the membrane in conformations characterized by asymmetric distribution of the hydrophobic and hydrophilic residues along the effective molecular surface. As a result, they can adopt complicated intramembrane shapes (Han et al., 2001) and oblique orientations (Brasseur et al., 1997; Peuvot et al., 1999) characterized by the angle of 30–60° between the molecular axis and the normal to the monolayer surface.

The aim of this work is to analyze by means of the elastic model of the lipid monolayer the behavior of fusion peptides embedded obliquely into the membrane matrix, to address the

Submitted February 11, 2004, and accepted for publication April 15, 2004.
Address reprint requests to Michael M. Kozlov, E-mail: michk@post.tau.ac.il.

0006-3495/04/08/999/14 $2.00
doi: 10.1529/biophysj.104.041467

type of membrane deformations induced by such inclusions, and to compute the membrane-mediated interaction between the inclusions. We show that although a priori one expects the oblique inclusion to induce a complicated monolayer deformation including perturbation of the orientation of the hydrocarbon chains, the model predicts that the deformation is, practically, limited by bending of a fragment of the monolayer surrounding the inclusion and the related rotation of the inclusion with respect to the membrane plane. The changes of chain orientation may become essential if the oblique inclusion is embedded into one monolayer of a lipid bilayer, whereas the second monolayer provides a considerable resistance to membrane bending. Analysis of this case is outside the scope of this study. The interinclusion interaction is predicted to have a character similar to the interaction of two-dimensional electric dipoles and qualitatively different from the interaction between the axisymmetric inclusions analyzed previously.

Statement of the problem

Our goal is to investigate the effects of the hydrophobic oblique inclusions on monolayer structure. The monolayer is subject to lateral tension, γ, and in the initial state preceding insertion of an inclusion it has a flat shape. The inclusion is modeled as an oblique circular cylinder, whose top base is hydrophilic and, therefore, located at the monolayer surface, whereas the side surface is hydrophobic and has to be inserted into the hydrocarbon moiety of the monolayer. The axis of the cylinder, represented by the unit vector $\vec{m}$, is inclined by the angle ζ with respect to the normal to the cylinder base $\vec{M}$ (Fig. 1). The embedded inclusion can induce bending of the monolayer and tilt of the hydrocarbon chains of lipid molecules with respect to the normal of the monolayer surface (Hamm and Kozlov, 2000).

We first determine the conformation of the monolayer that embeds one oblique inclusion. Based on this analysis we will consider the structure of a monolayer containing two oblique inclusions, and analyze the monolayer-mediated interaction between them. Our analysis will be based on the tilt and bending theory of monolayer deformations (Hamm and Kozlov, 2000).

The embedded inclusion can exert several effects on the lipid monolayer. One can distinguish between effects that depend on the shape of the inclusion and those that are general and not shape specific. One such general effect is related to the large thermal fluctuations in the shape of lipid membranes (Helfrich, 1990). The embedded inclusions modify these fluctuations and change the free energy of the membrane, resulting in interaction between the inclusions (Netz and Pincus, 1995; Goulian et al., 1993). Another general effect arises from the lipid chains in direct contact with the inclusion. The lipid chains cannot penetrate the rigid inclusion, and, therefore, many of their chain conformations are prohibited and the entropy of the chains decreases (Fattal and Benshaul, 1993). In this work we do not consider the general effects above and focus on effects resulting from the specific oblique shape of the inclusion. To this end we find the difference between the energy of a monolayer embedding oblique circular cylinders and the energy of the reference state, which consists of a monolayer embedding right circular cylinders.

THEORETICAL MODEL

Shape and orientation of the inclusion

The inclusion is modeled as an oblique circular cylinder (Fig. 1 *a*). The radius of the cylinder base is a, and its height is taken to be equal to the monolayer thickness. The inclusion shape is determined by the unit vector $\vec{M}$ normal to the top base and the unit vector $\vec{m}$ directed along the cylinder axis. The angle between the two vectors, denoted by ζ, will be called in this work the skew angle.

In the initial state the monolayer is flat (Fig. 1 *b*) but can be bent in the course of deformations, resulting in a change of the inclusion orientation (Fig. 1 *c*). To describe the system, we use a system of Cartesian coordinates, $\{x, y, z\}$, whose origin coincides with the center of the inclusion top base in the initial flat state (Fig. 1 *b*) of the membrane. The unit vectors of the Cartesian axes are denoted by $\{\hat{x}, \hat{y}, \hat{z}\}$. In the initial state (Fig. 1 *b*) the z axis points along the initial direction of $\vec{M}$ whereas the plane containing the $\vec{M}$ and $\vec{m}$ vectors forms the angle α with the x axis. After the deformation (Fig. 1 *c*), orientation of the inclusion is described by two more angles: the polar, θ_m, and azimuthal, β, angles determining the new orientation of the top base normal $\vec{M}$ with respect to the chosen Cartesian axes.

In the initial state, the cylinder orientation is given by

$$\vec{M} = \hat{z}; \quad \vec{m} = \cos\zeta\hat{z} + \sin\zeta(\cos\alpha\hat{x} + \sin\alpha\hat{y}). \qquad (1)$$

After the deformation the top base normal is represented by

$$\vec{M} = \sin\theta_m\cos\beta\hat{x} + \sin\theta_m\sin\beta\hat{y} + \cos\theta_m\hat{z}. \qquad (2)$$

The orientation of cylinder axis, $\vec{m}$, in the deformed state is given by a rather complicated relationship, which can be simplified if $\vec{m}$ deviates from $\vec{M}$ by a small angle, $\zeta \ll 1$. In this case, the monolayer deformations and the related change of the inclusion orientation expressed by the polar angle-θ_m

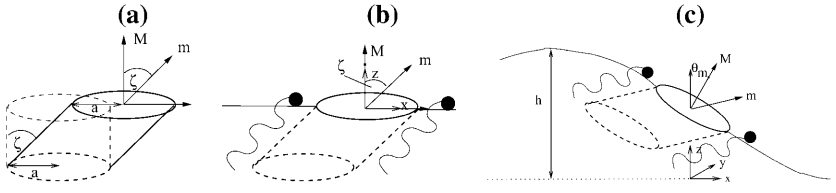

FIGURE 1 An oblique circular cylinder. (*a*) The oblique cylinder (*solid lines*) characterized by the skew angle ζ. $\vec{M}$ is the normal to the top base; $\vec{m}$ is the axis of the oblique cylinder. (*b*) The oblique cylinder embedded in a flat monolayer, with $\vec{M} = \hat{z}$. In this figure the orientation of the oblique cylinder is along the x axis, which means that $\alpha = 0$. (*c*) The monolayer undergoes bending deformation. $\vec{M}$ is reoriented in space, inclined by the polar angle θ_m with respect to $\hat{z}$ (β is not shown).

have to be small as well, $\theta_m \ll 1$, and the cylinder axis is given, approximately, by the equation

$$\vec{m} \approx \zeta \cdot (\cos\alpha \cdot \hat{x} + \sin\alpha \cdot \hat{y}) + \theta_m \cdot (\cos\beta \cdot \hat{x} + \sin\beta \cdot \hat{y}) + m_z \cdot \hat{z}\,, \quad (3)$$

where

$$m_z = 1 - (\zeta^2 + \theta_m^2 + 2 \cdot \zeta \cdot \theta_m \cdot \cos(\alpha - \beta))/2, \quad (4)$$

and that takes into account the contributions up to the second order in ζ and θ_m.

Elastic energy of the monolayer

The first contribution to the monolayer elastic energy is related to the deformations of tilt and splay of the hydrocarbon chains of lipid molecules. To account for this energy of the monolayer we use the elastic model presented in Hamm and Kozlov (2000) and further developed in Kozlovsky and Kozlov (2002). The monolayer is described by the shape of its neutral surface lying at the interface between the polar heads and the hydrocarbon chains (Leikin et al., 1996). It is represented by the height, $h(x, y)$, of the monolayer neutral surface above the $z = 0$ plane (Fig. 1 *c*). The normal to the surface is given by

$$\vec{N} = \frac{\hat{z} - \vec{\nabla}h}{\sqrt{1 + (\vec{\nabla}h)^2}}. \quad (5)$$

The average orientation of the hydrocarbon chains at each point of the monolayer surface is expressed by a unit vector $\vec{n}(x, y)$.

Three deformations contribute to the monolayer elastic energy. The first is tilt $\vec{t}$ of the chain orientation $\vec{n}$ with respect to the normal to the monolayer surface determined by

$$\vec{t} = \frac{\vec{n}}{\vec{n} \cdot \vec{N}} - \vec{N}. \quad (6)$$

The second and third are splay, $\tilde{J}$, and saddle splay, $\tilde{K}$, of the hydrocarbon chains. The latter deformations include additive contributions from the monolayer bending and tilt variation along the monolayer surface (Hamm and Kozlov, 2000). They can be expressed as the first and second order invariants of the tensor n_{ij}, which is a covariant gradient of the chain director $\vec{n}$ calculated along the monolayer surface (Appendix C). The splay is the covariant divergence of the chain director, $\tilde{J} = div\vec{n} = n_{ii}$, whereas the saddle splay is the determinant of the director gradient, $\tilde{K} = \det n_{ij}$ (Hamm and Kozlov, 2000; Kozlovsky and Kozlov, 2002). In the case of a bent monolayer with vanishing tilt, $\vec{t} = 0$, the splay and saddle splay reduce to the total, J, and Gaussian, K, curvatures of the monolayer surface (Hamm and Kozlov, 2000).

The structure of the monolayer is characterized by its spontaneous curvature, J_s, and by its saddle splay modulus, $\bar{\kappa}$ (Helfrich, 1973). The resistance of the monolayer to deformation is accounted by the monolayer bending, κ, and tilt, κ_t, moduli (Hamm and Kozlov, 1998, 2000). The elastic energy per monolayer unit area related to the reference state of a flat monolayer with vanishing tilt is given by

$$f = \frac{1}{2}\kappa\,(\tilde{J} - J_s)^2 + \bar{\kappa}\tilde{K} + \frac{1}{2}\kappa_t t^2 - \frac{1}{2}\kappa J_s^2. \quad (7)$$

Further contribution to the elastic energy is related to the monolayer lateral tension γ. Because the monolayer is undergoing bending deformation, its area, S, is larger than the projection area, A, onto the $x - y$ plane, along which acts the tension γ. The area element, dS, and the corresponding element of the projection area, dA, are related by

$$dS = \sqrt{1 + (\vec{\nabla}h)^2}\,dA, \quad (8)$$

where $\vec{\nabla}h$ is the two-dimensional gradient of the height calculated along the x-y plane.

The energy of tension related to monolayer bending is given by

$$F_{\text{tension}} = \gamma(S - A). \quad (9)$$

The total elastic energy related to reference state, which is characterized by vanishing deformations: $h(x, y) = 0$, $\vec{t}(x, y) = 0$, is expressed for the case of small deformations by

$$F = \iint \left[\frac{1}{2}\kappa(\tilde{J} - J_s)^2 + \bar{\kappa}\tilde{K} + \frac{1}{2}\kappa_t \vec{t}^{\,2} - \frac{1}{2}\kappa J_s^2 + \gamma\right] dS - \gamma A. \quad (10)$$

The energy of small deformations

We consider oblique inclusions whose shape deviates only slightly from a right circular cylinder, as determined by the condition $\zeta \ll 1$. The deformations of tilt, splay, and saddle splay of the lipid monolayer produced by such inclusions will be small as expressed by

$$|\vec{t}| \ll 1, \quad |\tilde{J}\delta| \ll 1, \quad \text{and } |\tilde{K}\delta^2| \ll 1, \quad (11)$$

where δ is the monolayer thickness. These conditions are prerequisites for the validity of the elastic model of tilt and splay deformations we are using (Hamm and Kozlov, 2000). Because the monolayer deforms only slightly with respect to the flat state, we also assume that the slope of the monolayer surface is small everywhere, $|\vec{\nabla}h| \ll 1$. Taking into account the contributions up to the second order in $|\vec{\nabla}h|$ and $|\vec{t}|$, the average orientation of the lipid chains, as derived from Eqs. 5 and 6, is presented by

$$\vec{n} = \frac{\vec{N} + \vec{t}}{\sqrt{1 + \vec{t}^{\,2}}} \approx \hat{z} - \vec{\nabla}h + \vec{t} - \hat{z} \cdot \left[\frac{1}{2} \cdot \vec{t}^{\,2} + \frac{1}{2} \cdot (\vec{\nabla}h)^2\right], \quad (12)$$

the splay of the lipid chains is given by

$$\tilde{J} = div\,\vec{n} \approx -\nabla^2 h + \vec{\nabla} \cdot \vec{t}, \quad (13)$$

where $\nabla^2 = (\partial^2/\partial x^2) + (\partial^2/\partial y^2)$, and the elastic energy (Eq. 10) has the form

$$F = \frac{1}{2}\iint [\kappa(-\nabla^2 h + \vec{\nabla} \cdot \vec{t} - J_s)^2 + \kappa_t \vec{t}^{\,2} + \bar{\kappa} \cdot \det(\vec{e}_i(\vec{e}_j\vec{\nabla})(\vec{t} - \vec{\nabla}h))) + \gamma(\vec{\nabla}h)^2 - \kappa J_s^2]dA, \quad (14)$$

where the integration is performed over the projection of the monolayer surface onto the $x - y$ plane, A. Note that deviation of tilt from the x-y plane contributes to higher than quadratic order terms to the energy and, hence, has to be neglected in Eq. 14. The energy of saddle splay deformation, is given in Eq. 14 by the terms proportional to $\bar{\kappa}$, as derived in Appendix C. It can be shown (Appendix C) that integral of this term over the membrane area vanishes so that it does not contribute either to the total energy of membrane

deformation or to the energy of interaction between the inclusions (Appendix C). Hence, we omit the saddle splay contribution in the calculations below.

Boundary conditions at the inclusion boundary

The inclusion inserted into the monolayer imposes several conditions on the lipid chains adjacent to its boundary. Because the inclusion is a circular cylinder, it is convenient to use polar coordinates, $\{r,\phi\}$, and the corresponding unit vectors, $\{\hat{r},\hat{\phi}\}$. We call ϕ the azimuthal angle to be consistent with previous sections. The origin of the coordinate system, $r=0$, is set at the center of the top base of the oblique circular cylinder. If the top base is inclined by the angle θ_m (Fig. 1 *c*; Eq. 2), its projection onto the $x-y$ plane will be an ellipse, described by

$$r^2 = a^2 - a^2 \sin^2\theta_m \cos^2(\phi-\beta), \tag{15}$$

but, because $\theta_m \ll 1$, within the accuracy up to the linear order in θ_m, the boundary between the monolayer and the inclusion in the *x-y* plane is a circle, $r=a$.

The monolayer must match the inclusion boundary. The height of the monolayer surface at the boundary of the inclusion that changes with the orientation of the inclusion base, $\vec{M}$ (Eq. 2), is

$$[h]_{r=a} = h_0 - a\theta_m \cos(\phi-\beta). \tag{16}$$

The parameter h_0 is the vertical displacement of the center of the inclusion top base. If the top base of the inclusion is not inclined, $\theta_m=0$, all points of the top base have the same height $h=h_0$. The values of the parameters h_0, θ_m, and β will be determined from energy minimization.

The boundary condition for lipid chains adjacent to the inclusion is that the chain orientation, $\vec{n}$, must be tangent to the inclusion surface. This condition can be expressed by

$$(\vec{n}-\vec{m})\cdot\hat{r} = 0. \tag{17}$$

Otherwise, a void is created between the inclusion surface and the lipid chains or alternatively, the lipid chains penetrate the inclusion. The explicit form of this boundary condition taking into account Eqs. 3 and 12 is given by

$$[-\partial_r h + t_r]_{r=a} = \zeta\cos(\phi-\alpha) + \theta_m\cos(\phi-\beta), \tag{18}$$

where t_r is the radial component of the tilt vector, $t_r = \vec{t}\cdot\hat{r}$. Both boundary conditions (Eqs. 16 and 18) are accurate up to quadratic order in ζ and θ_m.

Euler-Lagrange equations

We have to determine the distribution of height $h(x,y)$ and tilt $\vec{t}(x,y)$ along the monolayer surface, for which the elastic energy F adopts its minimal value. The energy variation presented in Appendix A results in the following Lagrange equations for $h(x,y)$ and $\vec{t}(x,y)$

$$\kappa\nabla^2(\nabla^2 h - \vec{\nabla}\cdot\vec{t}) - \gamma\nabla^2 h = 0 \tag{19a}$$

$$\kappa_t\vec{t} + \kappa\vec{\nabla}(\nabla^2 h - \vec{\nabla}\cdot\vec{t}) = 0, \tag{19b}$$

whose solutions have to satisfy the conditions

$$\int_0^{2\pi} d\phi[\partial_r h_L]_{r=a} = 0 \tag{20a}$$

$$\int_0^{2\pi} d\phi[(h_B + a\partial_r h_L)\cos\phi]_{r=a} = 0 \tag{20b}$$

$$\int_0^{2\pi} d\phi[(h_B + a\partial_r h_L)\sin\phi]_{r=a} = 0. \tag{20c}$$

The height function that satisfies these equations can be written as a sum of two parts,

$$h = h_B + h_L, \tag{21}$$

where h_L solves Laplace equation, $\nabla^2 h_L = 0$, and h_B solves Helmholtz equation, $\nabla^2 h_B = \lambda^{-2} h_B$. It is convenient to introduce the characteristic length of the system, λ, defined by

$$\lambda^2 = \frac{\kappa}{\kappa_t} + \frac{\kappa}{\gamma}. \tag{22}$$

The resulting solution of Euler-Lagrange equations for the height function, whose slope decays for large r, is

$$h = \underbrace{A_0 K_0(r/\lambda) + \sum_{n=1}^{\infty} A_n K_n(r/\lambda)\cos(n\phi-\phi_{a,n})}_{h_B} + \underbrace{B_0\log(r/r_b) + \sum_{n=1}^{\infty} B_n r^{-n}\cos(n\phi-\phi_{b,n})}_{h_L} \tag{23}$$

The terms including the modified Bessel functions $K_n(x)$ and multiplied by the arbitrary amplitudes A_n correspond to h_B, whereas the terms, which are multiplied by the arbitrary amplitudes B_n, correspond to h_L. The arbitrary constant angles are denoted by $\phi_{a,n}$ and $\phi_{b,n}$, and r_b is a constant length. These constants along with the amplitudes will be determined from the boundary conditions. The tilt function is derived from the component h_B of the height function,

$$\vec{t} = -\frac{\gamma}{\kappa_t}\vec{\nabla}h_B = -\frac{\gamma}{\kappa_t}\vec{\nabla}\left(\sum_{n=0}^{\infty} A_n K_n(r/\lambda)\cos(n\phi-\phi_{a,n})\right). \tag{24}$$

For functions that minimize the energy and satisfy the boundary conditions (Eqs. 16, 18, and 20), the expression for the energy (Eq. 14) can be simplified (Appendix A) and becomes

$$F = \frac{1}{2}a\gamma\zeta\int_0^{2\pi} d\phi[h_B\cos(\phi-\alpha)]_{r=a}. \tag{25}$$

Although the equations above are given for a single inclusion, they also apply for a monolayer containing several oblique inclusions. In this case, the boundary conditions (Eqs. 16, 18, and 20) apply independently to each inclusion and the energy (Eq. 25) consists of a sum of integrals over the boundaries of all inclusion.

RESULTS

A single inclusion: monolayer shape and the energy

In the case of one oblique inclusion embedded into the initially flat monolayer, the symmetry of the system requires that the solution is proportional to odd powers of $\cos(\phi-\alpha)$. Accordingly, the height (Eq. 23) and the tilt (Eq. 24) functions have the form

$$h=(B/r+AK_1(r/\lambda))\cos(\phi-\alpha)$$
$$\vec{t}=-A\gamma/\kappa_t\vec{\nabla}(K_1(r/\lambda)\cos(\phi-\alpha)). \quad (26)$$

Determination of the unknown constants A, B, and θ_m, based on Eqs. 20a, 20b, and 20c and the boundary conditions (Eqs. 16 and 18), result in

$$A=\frac{a\Gamma\zeta}{K_1(a/\lambda)},\quad B=a^2\Gamma\zeta,\quad \theta_m=-2\Gamma\zeta, \quad (27)$$

where the dimensionless parameter, Γ, is defined as

$$\Gamma=\left(3-\frac{(a/\lambda)K_1'(a/\lambda)}{K_1(a/\lambda)}(1+\gamma/\kappa_t)\right)^{-1}. \quad (28)$$

Γ decreases monotonically to zero as a function of growing a/λ or γ/κ_t, and approaches its maximum value, $\Gamma=1/4$ when $a/\lambda\to 0$ and $\gamma/\kappa_t\to 0$. The height of the monolayer embedding the oblique inclusion is determined by

$$h=a\zeta\Gamma\left(\frac{a}{r}+\frac{K_1(r/\lambda)}{K_1(a/\lambda)}\right)\cos(\phi-\alpha). \quad (29)$$

The base of the inclusion is inclined by the angle $\theta_m=-2\Gamma\zeta$ (Eqs. 2 and 27). A profile of a monolayer embedding an oblique inclusion is shown in Fig. 2.

The tilt of the hydrocarbon chains is given by

$$\vec{t}=\frac{\Gamma\zeta}{K_1(a/\lambda)}\frac{\gamma}{\kappa_t}\Big[-\frac{a}{\lambda}K_1'(r/\lambda)\cos(\phi-\alpha)\,\hat{r}+\frac{a}{r}K_1(r/\lambda)\sin(\phi-\alpha)\hat{\phi}\Big]. \quad (30)$$

The energy of a monolayer embedding a single oblique-cylindrical inclusion relative to the energy of embedding a right-cylindrical inclusion (Eq. 25) is given in the quadratic approximation in the skew angle ζ by

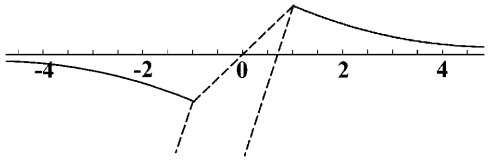

FIGURE 2 A cross section of the profile of a monolayer (*solid line*) embedding an oblique inclusion (*dashed lines*) for $\gamma\ll\kappa_t$ and $\lambda=5a$.

$$F=\frac{1}{2}\pi a^2\gamma\Gamma\zeta^2. \quad (31)$$

The energy must be en even function of ζ because changing $\zeta\to-\zeta$ is equivalent to rotating the inclusion orientation by π, $\alpha\to\alpha+\pi$ (Eq. 3). Therefore, the next order term of F will be proportional to ζ^4.

We now consider the realistic values of the parameters determining the monolayer shape, tilt, and energy (Eqs. 29–31). The tilt modulus was estimated to be $\kappa_t\approx 40\,\mathrm{mN/m}$ (Hamm and Kozlov, 1998). The maximal tension a lipid bilayer can sustain before it ruptures is about $\gamma_{bilayer}\approx 6\,\mathrm{mN/m}$ (the exact value depends on the lipid species and the time of experiment) (Evans and Needham, 1987) meaning that the maximal monolayer tension is about $\gamma_{max}=3\,\mathrm{mN/m}$. Therefore, in realistic lipid monolayers $\gamma\ll\kappa_t$, so that the characteristic decay length of membrane deformations (Eq. 22) becomes $\lambda\approx\sqrt{\kappa/\gamma}$. A typical cross section radius of a rod representing such membrane inclusion as α-helical peptide is about $a=1\,\mathrm{nm}$ (Macosko et al., 1997). Using this value we obtain that $\kappa/a^2\approx 40\,\mathrm{mN/m}\approx\kappa_t$, meaning that $(a/\lambda)^2\approx\gamma/\kappa_t$. Therefore, we have that both $\gamma/\kappa_t\ll 1$ and $a/\lambda\ll 1$, so that Γ can be taken at its maximal value $\Gamma=1/4$.

It follows from the above estimations that the slope of the surface is small everywhere, $|\vec{\nabla}h(\vec{r})|<\zeta/\sqrt{2}$, consistent with our approximation. The tilt function is smaller by the factor γ/κ_t than the height gradient, $\vec{\nabla}h$ (Eqs. 26 and 31). Because, as shown above, this factor is small, $\gamma/\kappa_t\ll 1$, the deformations of a monolayer produced by an oblique inclusion practically do not include tilt of the lipid chains. This is illustrated in Fig. 2 where we show the calculated height profile of such a monolayer embedding an oblique inclusion. Indeed, according to the figure, the monolayer contacts the inclusion boundary at a right angle, and, therefore, the lipid chains are not required to tilt. Hence, the monolayer bending is the major deformation resulting from embedding an oblique inclusion.

Interaction between two inclusions

We consider two oblique inclusions separated by a distance L, which is much larger than the inclusion radius, $L\gg a$. The skew angles of the inclusions are ζ_1 and ζ_2, and their orientations in the membrane plane are characterized by the azimuthal angles α_1 and α_2, which are determined with

respect to the axis x connecting the centers of the inclusion bases (Fig. 3). Our goal is to calculate the energy of the membrane-mediated interaction between the inclusions, F_{int}, as a function of their separation and orientation. The calculation presented in (Appendix C) and accounting for contributions up to third order in a/L and a/λ results in

$$F_{\text{int}} = \frac{\pi}{8}a^2\gamma\zeta_1\zeta_2\frac{a^2}{L^2}\left[\left(1 - 2\frac{L}{\lambda}K_1(L/\lambda)\right)\right.$$
$$\left.\times\cos(\alpha_1 + \alpha_2) - 2\frac{L^2}{\lambda^2}K_0(L/\lambda)\cos\alpha_1\cos\alpha_2\right]. \quad (32)$$

Simplified expressions for the interaction energy can be obtained for the two extreme interaction regimes determined by the ratio L/λ. For large separations, $L \gg \lambda$, the modified Bessel functions $K_n(L/\lambda)$ decay exponentially, so that the energy becomes

$$F_{\text{int}}(L \gg \lambda) \approx \frac{\pi}{8}a^2\gamma\zeta_1\zeta_2\frac{a^2}{L^2}\cos(\alpha_1 + \alpha_2). \quad (33)$$

In the opposite regime of $L \ll \lambda$ the argument of the modified Bessel functions is small. Using the approximate form of the modified Bessel functions for small argument

$$K_0(x\to 0) \approx -\ln x, \quad K_1(x\to 0) \approx 1/x, \quad (34)$$

the interaction energy becomes

$$F_{\text{int}}(L \ll \lambda) \approx -\frac{\pi}{8}a^2\gamma\zeta_1\zeta_2\frac{a^2}{L^2}\cos(\alpha_1 + \alpha_2). \quad (35)$$

The character of the interaction between the inclusions depends on the distance L between them and on their orientation with respect to the axis x connecting their centers as well as their mutual orientation, as determined by the sum of the azimuthal angles, $\alpha_1+\alpha_2$. It follows from Eqs. 33 and 35 that the interaction changes from repulsive to attractive or vice versa when the inclusions approach each other from long to short distances. The interaction is attractive at large and repulsive at small distances if $\pi/2<\alpha_1+\alpha_2<3\pi/2$. In case of orientations with $-\pi/2<\alpha_1+\alpha_2<\pi/2$ the interaction changes from repulsive at large separation to attractive at small one.

The energy change in the whole range of the interinclusion distances L is illustrated in Fig. 4 for four representative inclusion orientations. For convenience, the energy is represented in dimensionless form, F_{int}/Λ, where Λ is a factor accounting for all parameters of the system, which are independent on the inclusion separation and orientation,

$$\Lambda = \frac{\pi}{8}a^2\gamma\zeta_1\zeta_2\frac{a^2}{\lambda^2}, \quad (36)$$

and the distance is normalized by the characteristic length, L/λ.

Consider first the inclusions, which are directed oppositely but along the x axis direction. This corresponds to the cases where their azimuthal angles are $\alpha_1 = 0$ and $\alpha_2 = \pi$, what can be presented schematically by two arrows $\rightarrow\leftarrow$; or $\alpha_1 = \pi$ and $\alpha_2 = 0$ ($\leftarrow\rightarrow$). These two cases are illustrated in (Fig. 3, *b* and *c*), respectively. All other orientations of the particles mentioned below can be presented analogously. The interaction energy shown in Fig. 4 (*1*) represents attraction at large L, repulsion at small L, and a shallow minimum of $F_{\text{int}}/\Lambda = -0.03$ at $L/\lambda = 4.2$. The same character of interaction is predicted for two inclusions, which are directed parallel to each other but perpendicularly to the x axis (either $\uparrow\uparrow$ or $\downarrow\downarrow$), what corresponds to the $\alpha_1 = \alpha_2 = \pm\pi/2$. The energy profile illustrated in Fig. 4 (*2*), shows a minimum $F_{\text{int}}/\Lambda = -0.11$, which is deeper than

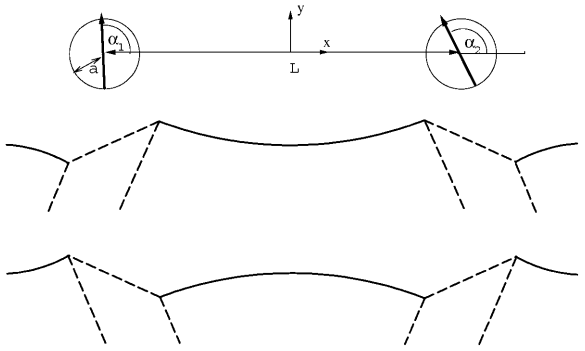

FIGURE 3 A view of the two oblique inclusions separated by a distance L. (*1*) The top view. The two thick arrows signify the directions of skewing of the two inclusions described by the azimuthal angle α. (*2*) A side view of two oppositely oriented inclusions with $\alpha_1 = 0$ and $\alpha_2 = \pi$. (*3*) A side view of two oppositely oriented inclusions with $\alpha_1 = \pi$ and $\alpha_2 = 0$.

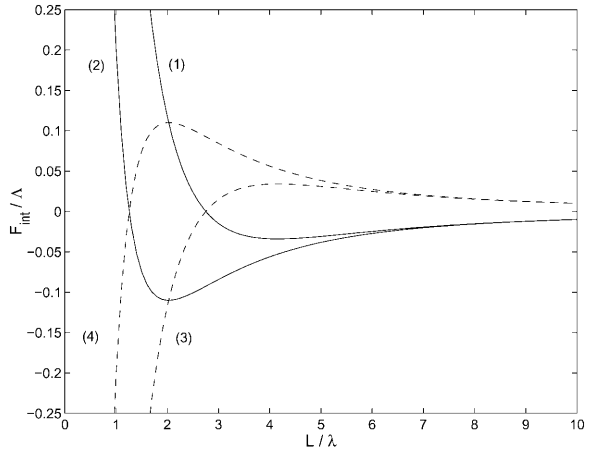

FIGURE 4 The normalized interaction energy, F_{int}/Λ, as a function of the separation, L/λ, for several orientations of the inclusions: (*1*) $\alpha_1 = \pi$, $\alpha_2 = 0$ or $\alpha_1 = 0$, $\alpha_2 = \pi$; (*2*) $\alpha_1 = \alpha_2 = \pm\pi/2$; (*3*) $\alpha_1 = \alpha_2 = 0$ or $\alpha_1 = \alpha_2 = \pi$; (*4*) $\alpha_1 = -\alpha_2 = \pm\pi/2$.

in the previous case, and is reached at smaller distances $L/\lambda = 2$.

A different behavior characterized by repulsion at large separation and attraction at small ones is predicted for the cases where the inclusions are oriented parallel to each other and to the x axis, as determined $\alpha_1 = \alpha_2 = 0$ ($\rightarrow\rightarrow$) or $\alpha_1 = \alpha_2 = \pi$ ($\leftarrow\leftarrow$) and illustrated in (Fig. 4 (*3*)); or the inclusion are antiparallel and directed perpendicularly to the x axis, as described by $\alpha_1 = -\alpha_2 = \pm\pi/2$ (either $\uparrow\downarrow$ or $\downarrow\uparrow$) and represented in (Fig. 4 (*4*)). In all these configurations, transition from the repulsion to attraction requires overcoming an energy barrier, which is larger in the case of antiparallel than parallel inclusions. Note that the two latter curves (Fig. 4 (*3* and *4*)) are mirror images of the two former ones (Fig. 4 (*1* and *2*)).

Summarizing the results presented in Fig. 4, the system reaches the state of the lowest energy when the two inclusions adopt the antiparallel orientation perpendicular to the x axis and approach each other to the closest distance (Fig. 4 (*4*)).

DISCUSSION

We addressed the elastic effects produced by insertion into a lipid monolayer of an amphiphilic inclusion modeling a fusion peptide. Our major goal was to investigate the effects resulting from obliqueness of the protein orientation within the membrane (Brasseur et al., 1997; Peuvot et al., 1999). Therefore, we modeled the peptide shape as a slanted cylinder and did not account for potentially more complicated forms such as a boomerang-like conformation, which has been observed for fusion peptide of a specific family of influenza virus hemagglutinins (Han et al., 2001). We have addressed the monolayer deformations resulting from accommodation of such inclusion in a way that its hydrophilic top base lies in the plane of the lipid polar heads, whereas the hydrophobic body resides in the hydrocarbon moiety of the monolayer. Based on this analysis, we have calculated the interaction between two oblique inclusions mediated by the monolayer deformations.

Because of a skewed shape of the inclusion, one could expect a priori that it generates deformation of tilt of the adjacent lipid hydrocarbon chains with respect to the monolayer surface and the related splay of the chains, the latter resulting from the tilt variation along the surface and from a possible monolayer bending. Our analysis based on the elastic model for tilt and splay deformation (Hamm and Kozlov, 2000) has demonstrated that for the realistic values of the monolayer elastic moduli an oblique inclusion is accommodated in the expense of the ''softest mode'' of deformation, which is the monolayer bending, whereas the chain tilt, practically, does not come into play. This result may have consequences for interpretation of the experimental results on orientation of inclusions, such as fusion peptides, inserted into lipid bilayers (Brasseur et al., 1997; Peuvot et al., 1999). It has to be taken into account that an apparent tilting of the peptides with respect to the membrane surface may result from local bending of the latter, while the axis of the insertion remains perpendicular to the membrane plane, as illustrated in Fig. 2.

It is important to note that our analysis does not include explicitly the effects of the second membrane monolayer, which is not penetrated by the oblique inclusion, but must undergo a bending deformation coupled to that of the inclusion containing monolayer. Bending resistance of the second monolayer increases the overall energy of the membrane curvature and may, therefore, favor some extent of the tilt deformation. According to our estimations, if the two monolayers have the value of bending rigidity of $\sim 10\,k_BT$, this effect is small and membrane bending remains the essential deformation. In a rare case where the second monolayer has a large bending rigidity or for an experimental setup where the oblique inclusion is inserted into a lipid monolayer attached to a rigid support, bending may be suppressed and the tilt of the hydrocarbon chains becomes the leading deformation.

Analysis of the interaction has shown that, depending on the orientation of the inclusions in the membrane plane, the interaction energy can have a minimum corresponding to an equilibrium interinclusion separation, or, alternatively, the inclusions tend to approach each other to zero distance after having overcome an energy barrier. The minimal final energy of the system corresponds to the latter case of the mutual approach to vanishing distance, which is accompanied by adopting the inclusions of an antiparallel orientation perpendicular to the axis connecting the centers of their bases.

An interesting feature of the interinclusion interaction is that at large separations it decays as $F_{int} \sim 1/L^2$ (Eq. 33). This scaling of the interaction energy differs from what has been found for other membrane-mediated interactions such as that originating from the ''hydrophobic mismatch'', which decays exponentially with the separation L (Aranda-Espinoza et al., 1996; Dan et al., 1993), or the interaction originating from the thermal shape fluctuations of the membrane decaying as $\sim 1/L^4$ (Goulian et al., 1993). This unusual $\sim 1/L^2$ decay can be understood by considering the formal analogy between the height of the monolayer surface, $h(x, y)$, and the electrical potential generated by two-dimensional dipoles. The height is the solution of the Euler-Lagrange equations (Eq. 19) and has two components (Eq. 23): h_B, satisfying the Helmholtz equation, $\nabla^2 h_B = \lambda^{-2} h_B$, and decaying exponentially at large distances, and h_L, which is the solution of the Laplace equation, $\nabla^2 h_L = 0$, and has a power law dependence. Hence, at large distances the component h_L will dominate. The boundary conditions at the inclusion boundary (Eqs. 16 and 18) have polar symmetry. According to both the Laplace equation and the symmetry, determination of h_L is similar, mathematically, to the electrostatic dipole problem. Indeed, it can be

easily shown that the interaction energy of two-dimensional dipoles is given by

$$U = -2\frac{p_1 p_2}{L^2}\cos(\alpha_1 + \alpha_2), \quad (37)$$

where p_1 and p_2 are the dipole moments, α_1 and α_2 are the angles between the dipole moments and the axis connecting them, and L is the distance between the dipoles. The electrostatic energy (Eq. 37) has the same scaling with the distance as the energy between the oblique inclusions. Interestingly, it can be shown that this analogy is valid also for small separations, $L \ll \lambda$ (Eq. 35).

Tension-free monolayers

In this work we have considered the monolayer subject to a lateral tensionγ, which, in addition to determining the elastic energy, suppresses the thermal undulation of the membrane. As a result, we did not have to address the issue of the undulation-mediated interaction between the inclusions, which plays a leading role in the case of stress-free membrane (Goulian et al., 1993). Although the real lipid monolayers are in most cases subject to some tension, it is important to mention shortly the predictions of our model for the case of $\gamma = 0$.

Our analysis shows that in the case of vanishing lateral tension, insertion of an oblique inclusion does not induce tilt deformation and the distribution of height of the monolayer surface generated by a single inclusion is given by

$$h = \frac{a^2\zeta}{2r}\cos(\phi - \alpha), \quad (38)$$

where r is the distance form the center of the inclusion top base and all other notations are the same as defined above.

The interaction energy between two oblique inclusions reduces to

$$F = \frac{1}{2}\kappa \iint [(\nabla^2 h + J_s)^2 - J_s^2]dA. \quad (39)$$

The corresponding Euler-Lagrange equations have been derived and solved in Weikl et al. (1998). Calculation of the interaction energy, F_{int}, by the method described above leads to

$$F_{int} = \pi\kappa\left(\frac{a}{L}\right)^6 [\zeta_1^2(2 + \cos^2\alpha_1) + \zeta_2^2(2 + \cos^2\alpha_2)]. \quad (40)$$

The interaction is always repulsive and decays with separation L much faster than the interaction in the presence of lateral tension (Eq. 33). Because of its fast decay $\sim 1/L^6$ the interaction (Eq. 40) can be neglected in comparison to the interaction mediated by the thermal membrane undulation, which has been calculated for two right circular cylinders (Goulian et al., 1993; Helfrich and Weikl, 2001; Park and Lubensky, 1996) and shown to scale as $1/L^4$.

CONCLUSION

It is commonly believed, that fusion proteins promote the fusion reaction by inserting into the target membrane and reducing the energy of fusion intermediates such as membrane stalks, hemifusion diaphragms, and fusion pores. Indeed, such action of the fusion proteins can be envisaged if one assumes that, in accord to their orientation inside the membranes, a fusion protein has an effective shape of oblique cylinder that promotes tilt of the hydrocarbon chains of lipid molecules. In this case, insertion of the fusion peptides into the fusion stalks could relieve the tilt of the chains, and fill the packing defect in the middle of the stalk and in the rim of the hemifusion diaphragm (Kozlovsky et al., 2002; Kozlovsky and Kozlov, 2002). However, the analysis above shows that an oblique cylindrical inclusion inserted into a lipid monolayer results in an anisotropic bending of the monolayer surface around the inclusion, but does not lead to tilt of hydrocarbon chains. According to our estimates, this monolayer bending cannot be the sole factor determining the membrane rearrangements. Therefore, the fusion peptides must have another property allowing them to drive the fusion reaction. This conclusion is consistent with data on mutations in the fusion peptide region that indicate a more specific role in fusion of the exact chemical side group of each amino acid in the fusion peptide conservative substitutions leading to changes in fusion phenotypes (Cross et al., 2001; Qiao et al., 1999). Possibly, the role of the fusion peptide is to create connections between the fusion proteins leading to formation of protein coats, which promote transformation of the early fusion intermediates into fusion pores (Chernomordik and Kozlov, 2003; Kozlov and Chernomordik, 2002). In addition, the membrane shape generated by a fusion peptide (Fig. 2) is reminiscent of the border between liquid ordered and disordered lipids domains. Perhaps the fusion peptide is designed as an oblique inclusion to reduce the line tension of lipid microdomains asymmetrically (in the outer cellular and viral leaflets only), and, hence, to stabilize the small size of microdomain needed for fusion.

APPENDIX A

In this section we derive the Euler-Lagrange equations and the related boundary conditions, solve these equations, and find a simple expression for the elastic energy of a monolayer.

Euler-Lagrange equations

The energy of a nearly flat monolayer with bending and tilt deformations is Eq. 14:

$$F = \frac{1}{2}\iint [\kappa(-\nabla^2 h + \vec{\nabla}\cdot\vec{t} - J_s)^2 + \kappa_t \vec{t}^{\,2} + \gamma(\vec{\nabla}h)^2 - \kappa J_s^2]dA. \tag{A1}$$

To derive the Euler-Lagrange equations, we consider small variations in the height of the monolayer surface, h, and the tilt of the hydrocarbon chains, $\vec{t}$. The variation in the energy resulting from the height variation, δh, is given by:

$$\delta F = \iint [\kappa(\nabla^2 h - \vec{\nabla}\cdot\vec{t} + J_s)\nabla^2\delta h + \gamma\vec{\nabla}h\cdot\vec{\nabla}\delta h]dA.$$

We manipulate the first term of the integrand

$$(\nabla^2 h - \vec{\nabla}\cdot\vec{t} + J_s)\nabla^2\delta h = \vec{\nabla}\cdot((\nabla^2 h - \vec{\nabla}\cdot\vec{t} + J_s)\vec{\nabla}\delta h) - \vec{\nabla}(\nabla^2 h - \vec{\nabla}\cdot\vec{t})\cdot\vec{\nabla}\delta h,$$

and obtain

$$\delta F = \iint [\kappa\vec{\nabla}\cdot((\nabla^2 h - \nabla\cdot\vec{t} + J_s)\vec{\nabla}\delta h) - (\kappa\vec{\nabla}(\nabla^2 h - \vec{\nabla}\cdot\vec{t}) - \gamma\vec{\nabla}h)\cdot\vec{\nabla}\delta h]dA.$$

The second term of the integrand can be presented in the form:

$$(\kappa\vec{\nabla}(\nabla^2 h - \vec{\nabla}\cdot\vec{t}) - \gamma\vec{\nabla}h)\cdot\vec{\nabla}\delta h = \vec{\nabla}\cdot[(\kappa\vec{\nabla}(\nabla^2 h - \vec{\nabla}\cdot\vec{t}) - \gamma\vec{\nabla}h)\delta h] - (\kappa\nabla^2(\nabla^2 h - \vec{\nabla}\cdot\vec{t}) - \gamma\nabla^2 h)\delta h,$$

leading to

$$\delta F = \iint [\vec{\nabla}\cdot[\kappa(\nabla^2 h - \vec{\nabla}\cdot\vec{t} + J_s)\vec{\nabla}\delta h - (\kappa\vec{\nabla}(\nabla^2 h - \vec{\nabla}\cdot\vec{t}) - \gamma\vec{\nabla}h)\delta h] + (\kappa\nabla^2(\nabla^2 h - \vec{\nabla}\cdot\vec{t}) - \gamma\nabla^2 h)\delta h]dA.$$

The first term of the integrand can be transformed into a boundary integral by the divergence theorem.

The variation in the energy resulting from the tilt variation, $\delta\vec{t}$, is given by:

$$\delta F = \iint [\kappa(-\nabla^2 h + \vec{\nabla}\cdot\vec{t} - J_s)\vec{\nabla}\cdot\delta\vec{t} + \kappa_t\vec{t}\cdot\delta\vec{t}]dA.$$

We present the first term of the integrand in the form

$$(-\nabla^2 h + \vec{\nabla}\cdot\vec{t} - J_s)\vec{\nabla}\cdot\delta\vec{t} = \vec{\nabla}\cdot((-\nabla^2 h + \vec{\nabla}\cdot\vec{t} - J_s)\delta\vec{t}) - \vec{\nabla}(-\nabla^2 h + \vec{\nabla}\cdot\vec{t})\cdot\delta\vec{t},$$

and obtain

$$\delta F = \iint [\kappa\vec{\nabla}\cdot((-\nabla^2 h + \vec{\nabla}\cdot\vec{t} - J_s)\delta\vec{t}) + (\kappa_t\vec{t} - \kappa\vec{\nabla}(-\nabla^2 h + \vec{\nabla}\cdot\vec{t}))\cdot\delta\vec{t}]dA.$$

The first integral can be transformed into a boundary integral by the divergence theorem. The variation in the energy to linear order when both the surface height and the tilt are varied is the sum of the two variations:

$$\delta F = \oint [\kappa(\nabla^2 h - \vec{\nabla}\cdot\vec{t} + J_s)(\vec{\nabla}\delta h - \delta\vec{t}) - (\kappa\vec{\nabla}(\nabla^2 h - \vec{\nabla}\cdot\vec{t}) - \gamma\vec{\nabla}h)\delta h]\cdot\hat{l}\,dl + \iint [(\kappa\nabla^2(\nabla^2 h - \vec{\nabla}\cdot\vec{t}) - \gamma\nabla^2 h)\delta h + (\kappa_t\vec{t} + \kappa\vec{\nabla}(\nabla^2 h - \vec{\nabla}\cdot\vec{t}))\cdot\delta\vec{t}]dA, \tag{A2}$$

where the line element of the boundary is dl and the normal to the boundary is $\hat{l}$. The condition for obtaining the energy minimum is that the first variation vanishes, $\delta F = 0$. The variations in the functions, δh and $\delta\vec{t}$, are arbitrary and independent. From the vanishing of the surface integral we obtain the Euler-Lagrange equations:

$$\kappa\nabla^2(\nabla^2 h - \vec{\nabla}\cdot\vec{t}) - \gamma\nabla^2 h = 0 \tag{A3a}$$

$$\kappa_t\vec{t} + \kappa\vec{\nabla}(\nabla^2 h - \vec{\nabla}\cdot\vec{t}) = 0. \tag{A3b}$$

We must also demand that the boundary integral vanishes (Eq. A2). We now specifically consider an oblique inclusion in a monolayer. The monolayer has one boundary around the inclusion and a second boundary far from the inclusion (at infinity). Because the deformations caused by the oblique inclusion are localized, at the far boundary they have to decay to zero so that the boundary integral vanishes. We are left with the boundary integral around the inclusion. The inclusion boundary is a circle. The boundary element is $dl = ad\phi$ and the normal to the boundary is $\hat{l} = -\hat{r}$. The boundary integral is set to be zero

$$\int_0^{2\pi} ad\phi[\kappa(\nabla^2 h - \vec{\nabla}\cdot\vec{t} + J_s)(-\partial_r\delta h + \delta t_r) + (\kappa\partial_r(\nabla^2 h - \vec{\nabla}\cdot\vec{t}) - \gamma\partial_r h)\delta h]_{r=a} = 0. \tag{A4}$$

The variations at the boundary, $[-\partial_r\delta h + \delta t_r]_{r=a}$ and $[\delta h]_{r=a}$ are not independent because they must satisfy the boundary conditions (Eqs. 16 and 18).

Solution of the Euler-Lagrange equations

The divergence of Eq. A3b can be presented as

$$\kappa_t\vec{\nabla}\cdot\vec{t} = -\kappa\nabla^2(\nabla^2 h - \vec{\nabla}\cdot\vec{t}),$$

its insertion into Eq. A3a results in

$$\kappa_t\vec{\nabla}\cdot\vec{t} = -\gamma\nabla^2 h,$$

and elimination $\vec{t}$ from Eq. A3a leads to

$$\kappa(1 + \gamma/\kappa_t)\nabla^2\nabla^2 h - \gamma\nabla^2 h = 0. \tag{A5}$$

We define the characteristic length of the system

$$\lambda^2 = \frac{\kappa}{\kappa_t} + \frac{\kappa}{\gamma},$$

so that the Eq. A5 adopts the form

$$\nabla^2\nabla^2 h - \lambda^{-2}\nabla^2 h = 0. \tag{A6}$$

One solution of the equation satisfies

$$\nabla^2 h = 0.$$

This is Laplace equation in two dimensions, whose solution in polar coordinates is

$$h_{\mathrm{L}} = A_0 + B_0 \log r + \sum_{\mathrm{n}=1}^{\infty} \Big(A_{\mathrm{n}} r^{\mathrm{n}} \cos(n\phi - \phi_{\mathrm{a,n}}) + B_{\mathrm{n}} r^{-\mathrm{n}} \cos(n\phi - \phi_{\mathrm{b,n}}) \Big),$$

where $\phi_{\mathrm{a,n}}$ and $\phi_{\mathrm{b,n}}$ are arbitrary constant angles. However, because we are interested only in surfaces with decaying slope, described by the asymptotic boundary condition $\vec{\nabla} h(r \to \infty) \to 0$, we retain only the corresponding terms

$$h_{\mathrm{L}} = B_0 \log(r/r_{\mathrm{b}}) + \sum_{\mathrm{n}=1}^{\infty} B_{\mathrm{n}} r^{-\mathrm{n}} \cos(n\phi - \phi_{\mathrm{b,n}}),$$

where r_{b} is a constant. To obtain the second solution of Eq. A6, we denote $\nabla^2 h = f$ and obtain

$$\nabla^2 f - \lambda^{-2} f = 0.$$

Solution of this equation can be presented as the sum of two parts,

$$h = h_{\mathrm{L}} + h_{\mathrm{B}},$$

where h_{L} is the solution of Laplace equation, $\nabla^2 h_{\mathrm{L}} = 0$, and h_{B} is the decaying solution of Helmholtz equation, $\nabla^2 h_{\mathrm{B}} = \lambda^{-2} h_{\mathrm{B}}$ having the form

$$h_{\mathrm{B}} = \sum_{\mathrm{n}=0}^{\infty} A_{\mathrm{n}} K_{\mathrm{n}}(r/\lambda) \cos(n\phi - \phi_{\mathrm{a,n}}),$$

where $K_{\mathrm{n}}(x)$ are the modified Bessel functions. The tilt is derived from h to be

$$\vec{t} = -\frac{\gamma}{\kappa_{\mathrm{t}}} \lambda^2 \vec{\nabla}(\nabla^2 h) = -\frac{\gamma}{\kappa_{\mathrm{t}}} \vec{\nabla} h_{\mathrm{B}}.$$

Concluding, the solution of Euler-Lagrange equations is

$$h = A_0 K_0(r/\lambda) + \sum_{\mathrm{n}=1}^{\infty} A_{\mathrm{n}} K_{\mathrm{n}}(r/\lambda) \cos(n\phi - \phi_{\mathrm{a,n}}) + B_0 \log r + \sum_{\mathrm{n}=1}^{\infty} B_{\mathrm{n}} r^{-\mathrm{n}} \cos(n\phi - \phi_{\mathrm{b,n}})$$

$$\vec{t} = -\frac{\gamma}{\kappa_{\mathrm{t}}} \vec{\nabla} \left(\sum_{\mathrm{n}=0}^{\infty} A_{\mathrm{n}} K_{\mathrm{n}}(r/\lambda) \cos(n\phi - \phi_{\mathrm{a,n}}) \right).$$

For h and $\vec{t}$ satisfying the Euler-Lagrange equations, the energy integral can be simplified. We present the energy (Eq. A1) as

$$F = \frac{1}{2} \iint \Big[\kappa(\nabla^2 h - \vec{\nabla} \cdot \vec{t} + J_{\mathrm{s}}) \nabla^2 h + \gamma \vec{\nabla} h \cdot \vec{\nabla} h + \kappa(-\nabla^2 h + \vec{\nabla} \cdot \vec{t} - J_{\mathrm{s}}) \vec{\nabla} \cdot \vec{t} + \kappa_{\mathrm{t}} \vec{t} \cdot \vec{t} \Big] dA + \frac{1}{2} \iint \Big[\kappa(\nabla^2 h - \vec{\nabla} \cdot \vec{t}) J_{\mathrm{s}} \Big] dA,$$

and perform the same derivation we used to calculate the first variation of the energy. As a result we obtain

$$F = \frac{1}{2} \oint \Big[\kappa(\nabla^2 h - \vec{\nabla} \cdot \vec{t} + 2J_{\mathrm{s}})(\vec{\nabla} h - \vec{t}) - (\kappa \vec{\nabla}(\nabla^2 h - \vec{\nabla} \cdot \vec{t}) - \gamma \vec{\nabla} h) h \Big] \cdot \hat{l} dl + \frac{1}{2} \iint \Big[(\kappa \nabla^2 (\nabla^2 h - \vec{\nabla} \cdot \vec{t}) - \gamma \nabla^2 h) h + (\kappa_{\mathrm{t}} \vec{t} + \kappa \vec{\nabla}(\nabla^2 h - \vec{\nabla} \cdot \vec{t})) \cdot \vec{t} \Big] dA,$$

where the surface integral vanishes and only the boundary integral contributes to the energy. The latter can be further simplified to

$$F = \frac{1}{2} \oint \Big[(\gamma h_{\mathrm{B}} + 2\kappa J_{\mathrm{s}})(\vec{\nabla} h - \vec{t}) + \gamma h \vec{\nabla} h_{\mathrm{L}} \Big] \cdot \hat{l} dl. \quad \text{(A7)}$$

Boundary conditions

The condition for vanishing of the boundary integral part of the variation (Eq. A4) can be written in a similar form as Eq. A7:

$$\int_0^{2\pi} d\phi [(h_{\mathrm{B}} + \kappa/\gamma J_{\mathrm{s}})(\partial_{\mathrm{r}} \delta h - \delta t_{\mathrm{r}}) + \partial_{\mathrm{r}} h_{\mathrm{L}} \delta h]_{\mathrm{r}=\mathrm{a}} = 0. \quad \text{(A8)}$$

The boundary condition (Eq. 16) contains three free parameters h_0, θ_{m} and β. They are found from the requirement that given an independent arbitrary variation of theses parameters, $\delta h_0, \delta \theta_{\mathrm{m}}$, and $\delta\beta$, the energy variation (Eq. A7) vanishes. The possible variation of the boundary condition (Eq. 16) is

$$[\delta h]_{\mathrm{r}=\mathrm{a}} = \delta h_0 - a \delta \theta_{\mathrm{m}} \cos(\phi - \beta) - a \theta_{\mathrm{m}} \sin(\phi - \beta) \delta\beta.$$

Instead, we can present it as

$$[\delta h]_{\mathrm{r}=\mathrm{a}} = \delta h_0 - a \delta \mu_1 \cos\phi - a \delta \mu_2 \sin\phi,$$

where $\delta\mu_1$ and $\delta\mu_2$ are linear combinations of $\delta\theta_{\mathrm{m}}$ and $\delta\beta$. The possible variation of the second boundary condition (Eq. 18) is

$$[-\partial_{\mathrm{r}} \delta h + \delta t_{\mathrm{r}}]_{\mathrm{r}=\mathrm{a}} = \delta \mu_1 \cos\phi + \delta \mu_2 \sin\phi.$$

Inserting the two last expressions into the condition (Eq. A7), we obtain,

$$\delta h_0 \int_0^{2\pi} d\phi [\partial_{\mathrm{r}} h_{\mathrm{L}}]_{\mathrm{r}=\mathrm{a}} - \delta\mu_1 \int_0^{2\pi} d\phi [(h_{\mathrm{B}} + a\partial_{\mathrm{r}} h_{\mathrm{L}}) \cos\phi]_{\mathrm{r}=\mathrm{a}} - \delta\mu_2 \int_0^{2\pi} d\phi [(h_{\mathrm{B}} + a\partial_{\mathrm{r}} h_{\mathrm{L}}) \sin\phi]_{\mathrm{r}=\mathrm{a}} = 0.$$

Because the three variations $\delta\mu_1$, $\delta\mu_2$, and δh_0 are independent, each of the three integrals must vanish, and we obtain the three conditions

$$\int_0^{2\pi} d\phi [\partial_{\mathrm{r}} h_{\mathrm{L}}]_{\mathrm{r}=\mathrm{a}} = 0$$

$$\int_0^{2\pi} d\phi [(h_{\mathrm{B}} + a\partial_{\mathrm{r}} h_{\mathrm{L}}) \cos\phi]_{\mathrm{r}=\mathrm{a}} = 0$$

$$\int_0^{2\pi} d\phi [(h_{\mathrm{B}} + a\partial_{\mathrm{r}} h_{\mathrm{L}}) \sin\phi]_{\mathrm{r}=\mathrm{a}} = 0.$$

Including these conditions and the boundary conditions (Eqs. 16 and 18), the energy (Eq. A7) can be further simplified

$$F = \frac{1}{2} a \gamma \zeta \int_0^{2\pi} d\phi [h_{\mathrm{B}} \cos(\phi - \alpha)]_{\mathrm{r}=\mathrm{a}}.$$

Appendix B

Interaction between two oblique inclusions

We first define for each inclusion a coordinate system whose origin is at the center of its top base. The polar coordinates are denoted r_1, ϕ_1 and r_2, ϕ_2, for the first and second inclusion, respectively. In both coordinate systems, the azimuthal angle ϕ is measured with respect to the direction from the first inclusion toward the second one. Thus, this direction is given by $\phi_1 = 0$ and also by $\phi_2 = 0$. The two oblique inclusions are slanted by the angles ζ_1 and ζ_2, called the skew angles, in the orientation of the azimuthal angles $\phi_1 = \alpha_1$ and $\phi_2 = \alpha_2$, respectively (Fig. 3).

We denote by $h^{(0)}(r, \phi)$ the solution for the height of the monolayer surface, h, determined by a single isolated inclusion (Eq. 29). The height resulting from two distant inclusions can be presented as a sum of the solutions for two isolated inclusions, $h_1^{(0)}(r_1, \phi_1) + h_2^{(0)}(r_2, \phi_2)$, with a small correction, $\delta h_1(r_1, \phi_1) + \delta h_2(r_2, \phi_2)$. Each correction $\delta h(r, \phi)$ is given by the full series (Eq. 23) and the total height is:

$$h = h_1^{(0)}(r_1, \phi_1) + h_2^{(0)}(r_2, \phi_2) + \delta h_1(r_1, \phi_1) + \delta h_2(r_2, \phi_2). \tag{B1}$$

The Laplace operator is invariant upon translation, $\nabla_1^2 h = \nabla_2^2 h$, where ∇_1^2 and ∇_2^2 denote differentiation with respect to the coordinates r_1, ϕ_1 and r_2, ϕ_2, respectively. Therefore, the height function satisfies the Euler-Lagrange equations (Eq. 19). Once the solution for the height is obtained, the tilt of the chains can be directly derived from it.

Boundary conditions

The solution (Eq. B1) must satisfy the boundary conditions around each inclusion. Due to the symmetry, it is sufficient to consider the boundary conditions around one of the inclusions. The function of the isolated solution, $h_1^{(0)}$, already satisfies the boundary conditions so we are interested only on how the correction function, denoted by Δh_1, is affected by the boundary conditions. The correction function is given by (Eq. B1)

$$\Delta h_1 = \delta h_1(r_1, \phi_1) + h_2^{(0)}(r_2, \phi_2) + \delta h_2(r_2, \phi_2).$$

Using Eq. 24, the boundary conditions (Eqs. 16 and 18) become

$$[\Delta h_1]_{r=a} = h_0 - a\theta_m \cos(\phi - \beta) \tag{B2a}$$

$$[\partial_r \Delta h_1 + (\gamma/\kappa_t)\partial_r \Delta h_{1B}]_{r=a} = -\theta_m \cos(\phi - \beta), \tag{B2b}$$

where Δh_{1B} is the component of Δh_1, which solves Helmholtz equation, $\nabla^2 h_{1B} = \lambda^{-2} h_{1B}$, whereas h_0, μ, β are free parameters to be set by the other boundary conditions. The general method of applying the boundary conditions is to expand the correction to the function, Δh_1, as a Fourier series (with coefficients that are functions of r) around the center of the first inclusion:

$$\begin{aligned}\Delta h_1 &= \delta h_1(r_1, \phi_1) + h_2^{(0)}(r_2, \phi_2) + \delta h_2(r_2, \phi_2) \\ &= \sum_{n=0}^{\infty} f_n(r_1)\cos(n\phi_1 - \xi_n).\end{aligned} \tag{B3}$$

The boundary conditions (Eqs. 20 and B2) are independent for each Fourier mode. We first consider the $n = 0$ term. It is given by (Eq. 23)

$$\begin{aligned}f_0(r_1) =& A_0 K_0(r_1/\lambda) + B_0 \log(r_1/r_b) \\ &+ \frac{1}{2\pi}\int_0^{2\pi} [h_2^{(0)} + \delta h_2]_{r_1=a} d\phi_1.\end{aligned} \tag{B4}$$

The boundary condition (Eq. 20a), which relates to the harmonic (i.e., a solution of Laplace equation) part of the function, h_L, is automatically satisfied. To prove it we denote by h_{2L} the harmonic component due to the second inclusion that satisfies $\nabla^2 h_{2L} = 0$. We integrate its Laplacian over the area of the first inclusion,

$$\begin{aligned}0 = \iint_{|r_1 \le a|} \nabla^2 h_{2L}\, dA = \iint_{|r_1 \le a|} \vec{\nabla} \cdot \vec{\nabla} h_{2L}\, dA = \\ \int_0^{2\pi} a\, d\phi_1 [\vec{\nabla} h_{2L} \cdot \hat{r}_1]_{r_1=a} = a\int_0^{2\pi} d\phi_1 [\partial_{r_1} h_{2L}]_{r_1=a}.\end{aligned}$$

To satisfy the boundary condition (Eq. 20a), we just exclude from $\delta h_1(r_1, \phi_1)$ the radial harmonic term, i.e., $B_0 = 0$ (Eq. B4). The radial part of the boundary condition (Eq. B2a) is easily satisfied by setting $h_0 = f_0(r_1 = a)$. The boundary condition (Eq. B2b), which does not have a radial term, sets an implicit constraint on the derivative of the radial component, $\partial_r f_0(r_1 = a)$. It can always be satisfied by choosing the correct amplitude A_0 (Eq. B4).

The first mode term, $n = 1$ (Eq. B3), is the most important because the energy of the system (Eq. 25) depends only on the term proportional to $\cos(\phi_1 - \alpha_1)$, and it is discussed below. The boundary conditions for higher modes, $n \ge 2$, state that the height function (Eq. B2a) f_n, and its derivative, $\partial_r f_n$, along with the contributions from the radial component of the tilt, vanish at $r_1 = a$ (Eqs. 18 and B2b).

The interaction energy

The first mode term (Eq. B3) is given by (Eq. 23)

$$\begin{aligned}f_1(r_1)\cos(\phi_1 - \xi) = AK_1(r_1/\lambda)\cos(\phi_1 - \phi_a) + B\cos(\phi_1 - \phi_b)/r_1 \\ + \cos\phi_1 \frac{1}{\pi}\int_0^{2\pi} \cos\phi_1 [h_2^{(0)} + \delta h_2]_{r_1=a} d\phi_1 + \sin\phi_1 \frac{1}{\pi}\int_0^{2\pi} \sin\phi_1 [h_2^{(0)} + \delta h_2]_{r_1=a} d\phi_1.\end{aligned} \tag{B5}$$

The second inclusion is assumed to be far from the first one. The solution $h_2^{(0)}(r_2, \phi_2)$ at the region of the first inclusion will be small, its correction $\delta h_2(r_2, \phi_2)$ will be even smaller, and, therefore, the latter can be neglected. Next, we write the height determined by the second inclusion, $h_2^{(0)}(r_2, \phi_2)$, using the coordinates of the first inclusion, r_1, ϕ_1. The origin of the first inclusion corresponds to the coordinates $r_2 = L$ and $\phi_2 = \pi$ of the second inclusion. We write the Cartesian coordinates corresponding to the polar coordinates r_1, ϕ_1 without a subscript:

$$x = r_1 \cos\phi_1 \quad \text{and} \quad y = r_1 \sin\phi_1.$$

The function $h_2^{(0)}(r_2, \phi_2)$ is approximated by the first terms of its Taylor series expansion around the origin of the first inclusion, $x = y = 0$ (the subscripts $i, j, k = 1, 2$ denote the two coordinates x and y):

$$\begin{aligned}h_2^{(0)} = h_2^{(0)}\Big|_{r_2=L, \phi_2=\pi} + x_i \frac{\partial}{\partial x_i} h_2^{(0)} + \frac{1}{2} x_i x_j \frac{\partial^2}{\partial x_i \partial x_j} h_2^{(0)} \\ + \frac{1}{6} x_i x_j x_k \frac{\partial^3}{\partial x_i \partial x_j \partial x_k} h_2^{(0)} + \ldots.\end{aligned} \tag{B6}$$

We now analyze the magnitude of each term. The expansion is at the inclusion boundary, $r_1 = a$, where the Cartesian coordinates have similar magnitude, $x, y \sim a$. The magnitude of the derivatives is $\partial/\partial x_i \sim 1/L$ or $1/\lambda$ (Eq. 29). Therefore, the magnitude of each term is changed by a factor of a/L or a/λ. We assume that both factors are small, so the function is well approximated by the leading order terms. The energy of the system (Eq. 25) depends only on the terms proportional to $\cos(\phi_1 - \alpha_1)$. Such terms appear in the Taylor expansion (Eq. B6) only in odd powers. Therefore, the first order term is the first that contributes to the interaction energy, whereas the next contributing term is the third one, which is smaller by a factor of $(a/L)^2$ or $(a/\lambda)^2$. Note that the derivatives can be expressed through the coordinates r_2, ϕ_2:

$$\frac{\partial}{\partial x}h_2^{(0)} = -\frac{\partial}{\partial r_2}h_2^{(0)}\bigg|_{r_2=L,\phi_2=\pi} \text{ and } \frac{\partial}{\partial y}h_2^{(0)} = -\frac{1}{L}\frac{\partial}{\partial \phi_2}h_2^{(0)}\bigg|_{r_2=L,\phi_2=\pi}.$$

Concluding, the first mode correction is (Eqs. B5 and B6)

$$f_1(r_1)\cos(\phi_1 - \xi) \approx AK_1(r_1/\lambda)\cos(\phi_1 - \phi_a) + \frac{B}{r_1}\cos(\phi_1 - \phi_b) + r_1\cos\phi_1\frac{\partial}{\partial x}h_2^{(0)} + r_1\sin\phi_1\frac{\partial}{\partial y}h_2^{(0)}.$$

There are four parameters, A, B, ϕ_a, and ϕ_b, which are fixed by the boundary conditions (Eq. B2) and by the conditions for vanishing variation at the boundary (Eqs. 20b and 20c).

Provided the first mode correction is determined, the energy is simply given by integrating (Eq. 25) around the boundary of the first inclusion. Another symmetric contribution to the interaction energy arises from the correction function near the second inclusion. It can be easily derived from the result of the calculation above by interchanging the subscripts 1 and 2. Finally, we obtain that the interaction energy, F_{int}, is:

$$F_{int} = \pi a^2\gamma\zeta_1\zeta_2\Gamma^2\left(2\left(\frac{a}{L}\right)^2\cos(\alpha_1 + \alpha_2) - \left(\frac{\gamma}{\kappa_t} + \frac{1}{\Gamma}\right)\frac{a/\lambda}{K_1(a/\lambda)}\left[\frac{1}{L/\lambda}K_1(L/\lambda)\cos(\alpha_1 + \alpha_2) + K_0(L/\lambda)\cos\alpha_1\cos\alpha_2\right]\right).$$

The derivation of the interaction energy was based on two approximations:

1. We took only the first order term of the Taylor expansion (Eq. B6). The next relevant term is smaller by a factor of $(a/L)^2$ or $(a/\lambda)^2$.
2. We neglected the correction to the function of the second inclusion, $\delta h_2(r_2, \phi_2)$ (Eq. B5). Its relative magnitude is $\delta h_2/h_2^{(0)} \sim (a/L)^2$ or $(a/\lambda)^2$.

Therefore, the next terms of the interaction energy are smaller by factors of $(a/L)^2$ and $(a/\lambda)^2$. Realistic monolayers are characterized by $\gamma \ll \kappa_t$, corresponding to $\Gamma \approx 1/4$. Using also the approximate form of the modified Bessel functions for a small argument (Eq. 34), the interaction energy F_{int} can be simplified to the expression Eq. 32.

Appendix C

Saddle splay deformation

In this section we calculate the energy contribution of the saddle splay deformation of the lipid chains, $\tilde{K}$, of a monolayer embedding an oblique inclusion. The saddle splay energy is given by (Eq. 10)

$$F_g = \bar{\kappa}\iint \tilde{K}dS. \quad \text{(C1)}$$

We first obtain the general expression for the saddle splay deformation, $\tilde{K}$, which quantifies a specific spatial variation of the vector function $\vec{n}$. To describe the spatial variations, we define two orthogonal directions in the monolayer surface, represented by two orthogonal unit vectors, $\vec{e}_1$ and $\vec{e}_2$. The chain orientation tensor, n_{ij}, is defined as

$$n_{ij} = \vec{e}_i \cdot ((\vec{e}_j \cdot \vec{\nabla})\vec{n}).$$

The saddle splay deformation is the determinant of the tensor, $\tilde{K} = \det(n_{ij})$ (Hamm and Kozlov 2000).

Next, we find an expression for $\tilde{K}$ in a monolayer whose slope is small. It proves useful to define the vector

$$\vec{v} = -\vec{\nabla}h + \vec{t}.$$

The chain orientation is given approximately by $\vec{n} \approx \hat{z} + \vec{v}$ (Eq. 12). The chain orientation tensor becomes

$$n_{ij} \approx \vec{e}_i \cdot ((\vec{e}_j \cdot \vec{\nabla})\vec{v}) \equiv v_{ij},$$

and the saddle splay deformation becomes $\tilde{K} \approx \det(v_{ij})$. In a monolayer whose slope is small, the polar unit vectors approximate the two orthogonal directions, $\vec{e}_1 \approx \hat{r}$ and $\vec{e}_2 \approx \hat{\phi}$. Given the vector $\vec{v}$ in polar coordinates, $\vec{v} = v_r(r, \phi)\hat{r} + v_\phi(r, \phi)\hat{\phi}$, the tensor v_{ij} is

$$v_{ij} = \begin{pmatrix} \partial_r v_r & (\partial_\phi v_r - v_\phi)/r \\ \partial_r v_\phi & (\partial_\phi v_\phi + v_r)/r \end{pmatrix},$$

where it was taken into account that $\partial_\phi \hat{r} = \hat{\phi}$. The saddle splay deformation is

$$\tilde{K} \approx \det(v_{ij}) = \frac{1}{r}\partial_r v_r(\partial_\phi v_\phi + v_r) - \frac{1}{r}\partial_r v_\phi(\partial_\phi v_r - v_\phi).$$

We calculate F_g for a monolayer whose slope is everywhere small, $|\vec{\nabla}h| \ll 1$. The energy integral (Eq. C1) becomes

$$F_g = \iint \bar{\kappa}\tilde{K}dS \approx \iint \bar{\kappa}\tilde{K}dA \approx \bar{\kappa}\int_a^\infty dr\int_0^{2\pi} rd\phi\det(v_{ij}).$$

The saddle splay term can be integrated to give a boundary integral

$$F_g = -\bar{\kappa}\int_0^{2\pi} d\phi\left[v_r\frac{\partial v_\phi}{\partial \phi} + \frac{1}{2}v_r^2 + \frac{1}{2}v_\phi^2\right]_{r=a}. \quad \text{(C2)}$$

The case of vanishing tilt

We first consider the saddle splay of a monolayer without tilt deformation, $\vec{t} = 0$, so that $\vec{v} = -\vec{\nabla}h$. The boundary conditions (Eqs. 16 and 18) fix $\vec{v}$ at the boundary to be

$$[v_\phi]_{r=a} = -\frac{1}{a}\left[\frac{\partial h}{\partial \phi}\right]_{r=a} = -\theta_m\sin(\phi - \beta)$$

$$[v_r]_{r=a} = -[\partial_r h]_{r=a} = \zeta\cos(\phi - \alpha) + \theta_m\cos(\phi - \beta).$$

Inserting these relations in Eq. C2, we obtain the saddle splay energy

$$F_g = -\frac{\pi}{2}\bar{\kappa}\zeta^2.$$

It is fixed by the shape of the inclusion and does not depend on the details of the monolayer deformation.

The case of nonvanishing tilt

We now consider a monolayer with both height and tilt deformations. The boundary condition (Eq. 18) sets the radial component of $\vec{v}$ at the boundary to have the form:

$$[v_r]_{r=a} = A\cos(\phi - \phi_0).$$

Because the trigonometric functions are orthogonal, only the first term of a Fourier series of v_ϕ will contribute to the integral (Eq. C2). We write this first term, denoted by v_ϕ^1, in a general form,

$$[v_\phi^1]_{r=a} = B\cos(\phi - \phi_b).$$

Using these v_r and v_ϕ we obtain that the energy related to the saddle splay deformation (Eq. C2) is

$$F_g = -\bar{\kappa}\pi\left(\frac{1}{2}A^2 + \frac{1}{2}B^2 - AB\sin(\phi_0 - \phi_b)\right).$$

The saddle splay modulus is expected to be negative (Templer et al., 1998). Therefore, the energy is nonnegative, $F_g \geq 0$, and attains its minimal value, $F_g = 0$, when $A = B$ and $\phi_0 - \phi_b = \pi/2$, meaning that $\left[v_\phi^1\right]_{r=a} = -A\sin(\phi - \phi_0)$. It is not obvious that v_ϕ can satisfy the latter condition to minimize the energy. But v_ϕ has two contributions, $v_\phi = -\partial_\phi h/a + t_\phi$. The tangential component of the tilt, t_ϕ, is not fixed by any boundary conditions, and we can set its value in order that v_ϕ will minimize the energy, resulting in

$$F_g = 0.$$

The last result is subtle. At first glance, it seems that t_ϕ is not free at the boundary, because for $r > a$, we have already found $\vec{t}(\vec{r})$ from the Euler-Lagrange equations. However, at the boundary, $r = a$, t_ϕ does not have to be a continuous function of the radial distance r,

$$\lim_{r\to a} t_\phi(r,\phi) \neq t_\phi(a,\phi),$$

and we are free to set its value on the boundary of the inclusion to minimize the saddle splay energy, regardless of its value in the monolayer. A discontinuous function has a δ-function derivative and, usually, contributes an infinite term to the energy. However, our energy expression (Eq. 14) does not contain the derivative $\partial t_\phi/\partial r$ and therefore the tangential component, t_ϕ, does not have to be continuous. The monolayer energy per unit area (Eq. 7) is a quadratic approximation. Addition of higher order terms containing the derivative $\partial t_\phi/\partial r$, such as $\tilde{K}^2$, will force t_ϕ to be continuous.

We are grateful to Moshe Schwartz for helpful discussion.

The work of M.M.K. is supported by the Human Frontier Science Program Organization, Israel Science Foundation (grant 75-03), and The Binational U.S.A.-Israel Science Foundation.

REFERENCES

Aranda-Espinoza, H., A. Berman, N. Dan, P. Pincus, and S. Safran. 1996. Interaction between inclusions embedded in membranes. *Biophys. J.* 71: 648–656.

Bohinc, K., V. Kralj-Iglic, and S. May. 2003. Interaction between two cylindrical inclusions in a symmetric lipid bilayer. *J. Chem. Phys.* 119:7435–7444.

Brasseur, R., T. Pillot, L. Lins, J. Vandekerckhove, and M. Rosseneu. 1997. Peptides in membranes: tipping the balance of membrane stability. *Trends Biochem. Sci.* 22:167–171.

Chernomordik, L. V., and M. M. Kozlov. 2003. Protein-lipid interplay in fusion and fission of biological membranes. *Annu. Rev. Biochem.* 72:175–207.

Cohen, F. S., and G. B. Melikyan. 2001. Implications of a fusion peptide structure. *Nat. Struct. Biol.* 8:653–655.

Cross, K. J., S. A. Wharton, J. J. Skehel, D. C. Wiley, and D. A. Steinhauer. 2001. Studies on influenza haemagglutinin fusion peptide mutants generated by reverse genetics. *EMBO J.* 20:4432–4442.

Dan, N., P. Pincus, and S. A. Safran. 1993. Membrane-induced interactions between inclusions. *Langmuir.* 9:2768–2771.

Davies, S. M., R. F. Epand, J. P. Bradshaw, and R. M. Epand. 1998. Modulation of lipid polymorphism by the feline leukemia virus fusion peptide: implications for the fusion mechanism. *Biochemistry.* 37:5720–5729.

Epand, R. M. 1998. Lipid polymorphism and protein-lipid interactions. *Biochim. Biophys. Acta.* 1376:353–368.

Epand, R. M., and R. F. Epand. 1994. Relationship between the infectivity of influenza virus and the ability of its fusion peptide to perturb bilayers. *Biochem. Biophys. Res. Commun.* 202:1420–1425.

Epand, R. F., I. Martin, J. M. Ruysschaert, and R. M. Epand. 1994. Membrane orientation of the SIV fusion peptide determines its effect on bilayer stability and ability to promote membrane fusion. *Biochem. Biophys. Res. Commun.* 205:1938–1943.

Evans, E., and D. Needham. 1987. Physical-properties of surfactant bilayer-membranes: thermal transitions, elasticity, Rigidity, cohesion, and colloidal interactions. *J. Phys. Chem.* 91:4219–4228.

Fattal, D. R., and A. Ben-Shaul. 1993. A molecular model for lipid-protein interaction in membranes: the role of hydrophobic mismatch. *Biophys. J.* 65:1795–1809.

Fattal, D. R., and A. Ben-Shaul. 1995. Lipid chain packing and lipid-protein interaction in membranes. *Physica A.* 220:192–216.

Fournier, J. B. 1999. Microscopic membrane elasticity and interactions among membrane inclusions: interplay between the shape, dilation, tilt and tilt-difference modes. *European Physical Journal B.* 11:261–272.

Goulian, M. 1996. Inclusions in membranes. *Curr. Opin. Colloid Interf. Sci.* 1:358–361.

Goulian, M., R. Bruinsma, and P. Pincus. 1993. Long-range forces in heterogeneous fluid membranes. *Europhys. Lett.* 22:145–150.

Hamm, M., and M. Kozlov. 1998. Tilt model of inverted amphiphilic mesophases. *European Physical Journal B.* 6:519–528.

Hamm, M., and M. Kozlov. 2000. Elastic energy of tilt and bending of fluid membranes. *European Physical Journal E.* 3:323–335.

Han, X., J. H. Bushweller, D. S. Cafiso, and L. K. Tamm. 2001. Membrane structure and fusion-triggering conformational change of the fusion domain from influenza hemagglutinin. *Nat. Struct. Biol.* 8:715–720.

Helfrich, W. 1973. Elastic properties of lipid bilayers: theory and possible experiments. *Z. Naturforsch.* 28c:693–703.

Helfrich, W. 1990. Elasticity and thermal undulations of fluid films of amphiphiles. *In* Liquids at Interfaces. J. Charvolin, J. F. Joanny, and J. Zinn-Justin, editors. Elsevier Science Publishers B.V., Amsterdam, The Netherlands.

Helfrich, W., and T. R. Weikl. 2001. Two direct methods to calculate fluctuation forces between rigid objects embedded in fluid membranes. *European Physical Journal E.* 5:423–439.

Huang, H. W. 1986. Deformation free energy of bilayer membrane and its effect on gramicidin channel lifetime. *Biophys. J.* 50:1061–1070.

Kozlov, M. M., and L. V. Chernomordik. 2002. The protein coat in membrane fusion: lessons from fission. *Traffic.* 3:256–267.

Kozlovsky, Y., L. V. Chernomordik, and M. M. Kozlov. 2002. Lipid intermediates in membrane fusion: formation, structure, and decay of hemifusion diaphragm. *Biophys. J.* 83:2634–2651.

Kozlovsky, Y., and M. Kozlov. 2002. Stalk model of membrane fusion: solution of energy crisis. *Biophys. J.* 88:882–895.

Leikin, S., M. M. Kozlov, N. L. Fuller, and R. P. Rand. 1996. Measured effects of diacylglycerol on structural and elastic properties of phospholipid membranes. *Biophys. J.* 71:2623–2632.

Macosko, J. C., C.-H. Kim, and Y.-K. Shin. 1997. The membrane topology of the fusion peptide region of influenza hemagglutinin determined by spin-labeling EPR. *J. Mol. Biol.* 267:1139–1148.

Netz, R. R., and P. Pincus. 1995. Inhomogeneous fluid membranes: segregation, ordering, and effective rigidity. *Phys. Rev. E. Stat. Phys. Plasmas Fluids Relat. Interdiscip. Topics.* 52:4114–4128.

Park, J. M., and T. C. Lubensky. 1996. Interactions between membrane inclusions on fluctuating membranes. *Journal De Physique I.* 6:1217–1235.

Peuvot, J., A. Schanck, L. Lins, and R. Brasseur. 1999. Are the fusion processes involved in birth, life and death of the cell depending on tilted insertion of peptides into membranes? *J. Theor. Biol.* 198:173–181.

Qiao, H., R. T. Armstrong, G. B. Melikyan, F. S. Cohen, and J. M. White. 1999. A specific point mutant at position 1 of the influenza hemagglutinin fusion peptide displays a hemifusion phenotype. *Mol. Biol. Cell.* 10:2759–2769.

Sackmann, E. 1995. Biological membranes architecture and function. In: Structure and Dynamics of Membranes. R. Lipowsky and E. Sackmann, editors. Elsevier, Amsterdam, The Netherlands. 1–64.

Skehel, J. J., and D. C. Wiley. 2000. Receptor binding and membrane fusion in virus entry: the influenza hemagglutinin. *Annu. Rev. Biochem.* 69:531–569.

Templer, R. H., B. J. Khoo, and J. M. Seddon. 1998. Gaussian curvature modulus of an amphiphilic monolayer. *Langmuir.* 14:7427–7434.

Weikl, T. R., M. M. Kozlov, and W. Helfrich. 1998. Interaction of conical membrane inclusions: effect of lateral tension. *Phys. Rev. E.* 57:6988–6995.